J Therm Anal Calorim (2012) 109:81–88
DOI 10.1007/s10973-011-1745-9

Thermal decomposition of $Ln(C_2H_5CO_2)_3 \cdot H_2O$ (Ln = Ho, Er, Tm and Yb)

J.-C. Grivel

Received: 4 February 2011 / Accepted: 15 June 2011 / Published online: 2 July 2011

Abstract The thermal decomposition of Ho(III), Er(III), Tm(III) and Yb(III) propionate monohydrates in argon was studied by means of thermogravimetry (TG), differential thermal analysis (DTA), IR-spectroscopy and X-ray diffraction (XRD). Dehydration takes place around 90 °C. It is followed by the decomposition of the anhydrous propionates to $Ln_2O_2CO_3$ (Ln = Ho, Er, Tm or Yb) with the evolution of CO_2 and 3-pentanone ($C_2H_5COC_2H_5$) between 300 and 400 °C. The further decomposition of $Ln_2O_2CO_3$ to the respective sesquioxides Ln_2O_3 is characterized by an intermediate plateau extending from approximately 500–700 °C in the TG traces. This stage corresponds to an overall composition of $Ln_2O_{2.5}(CO_3)_{0.5}$ but is more probably a mixture of $Ln_2O_2CO_3$ and Ln_2O_3. The stability of this intermediate state decreases for the lighter rare-earth (RE) compounds studied. Full conversion to Ln_2O_3 is achieved at about 1,100 °C. The overall thermal decomposition behaviour of the title compounds is similar to that previously reported for $Lu(C_2H_5CO_2)_3 \cdot H_2O$.

Keywords Rare-earth propionate · Holmium · Erbium · Thulium · Ytterbium · Thermal decomposition · TG/DTA · IR · X-ray powder diffraction

Introduction

The worldwide ongoing research and the development activities aiming at producing high critical current density superconducting tapes with the so-called coated-conductor architecture have initiated a strong interest in chemical solution processing of rare-earth (RE) containing compounds in the form of highly textured thin films [1, 2]. Among numerous potential precursors, RE propionates appear as promising candidates for the manufacture of the $REBa_2Cu_3O_7$ superconducting layers [3–8] as well as some buffer layers consisting of (La,Sr)MnO_3, $La_2Zr_2O_7$, $Gd_2Zr_2O_7$ or $Ce(Gd)O_{2-\delta}$, for example [9–12]. The achievement of high-performance-coated conductor tapes critically depends on the quality of the various constituent layers [13, 14] and optimisation of the processing parameters relies thus on a sound understanding and control of the thermal decomposition process of the precursor solutions.

A detailed interpretation of studies dealing with the decomposition process of propionate-based mixtures is rather difficult owing to the overlapping decomposition steps taking place in the individual propionates and interferences between the decomposition products as well as other salts like e.g. Ba-trifluoroacetate [7]. Clearly, a better understanding of the processes at play in these complex systems necessitates a sound knowledge of the thermal decomposition behaviour of the individual components. In relation with superconductor processing, detailed studies of the conversion of Cu-propionate into CuO and of the thermal decomposition of Ba-propionate have been published by Kaddouri et al. [15] and by Gobert-Ranchoux and Charbonnier [16], respectively. In contrast, only few studies devoted to the thermal decomposition behaviour of RE propionates have been published to date. $La(C_3H_5O_2)_3 \cdot H_2O$ and $Lu(C_3H_5O_2)_3 \cdot H_2O$ were reported to decompose to La_2O_3 and Lu_2O_3, respectively, via dehydration and formation of an intermediate RE oxycarbonate [17–19]. Beside these similarities in the decomposition

J.-C. Grivel (✉)
Materials Research Division, Risø National Laboratory for Sustainable Energy, Technical University of Denmark, 4000 Roskild, Denmark
e-mail: jean@risoe.dtu.dk

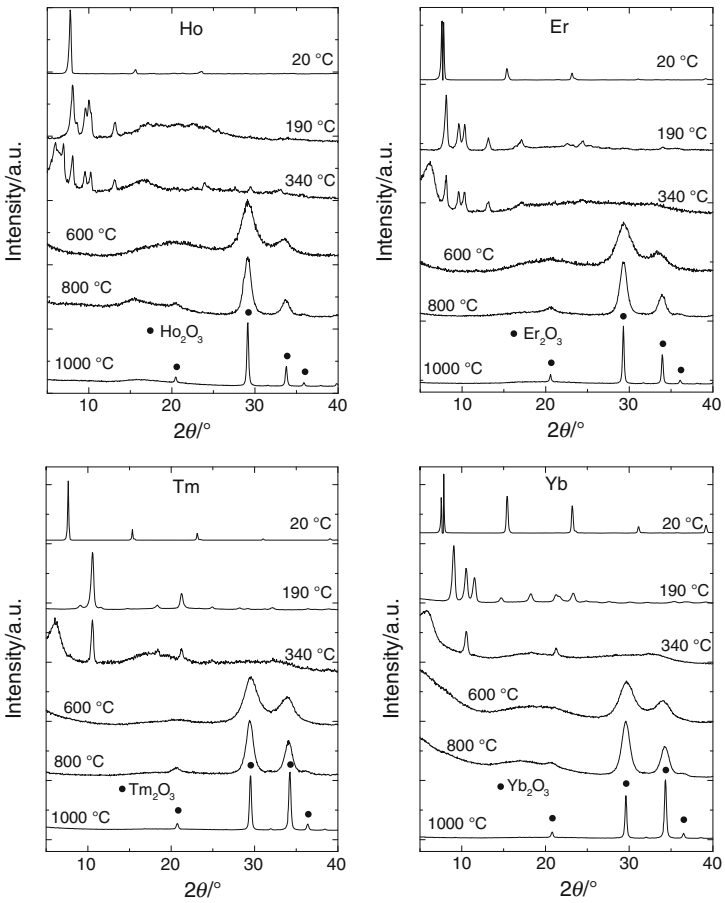

Fig. 1 XRD patterns recorded on the starting $Ln(C_2H_5CO_2)_3{\cdot}H_2O$ powders (20 °C) and on samples heated in the DTA/TG device at 5 K min^{-1} up to the indicated temperatures and fast cooled to room temperature. The apparent splitting of the low angle peak ($2\theta \approx 7.5°$) for Ln = Er and Yb is an artefact due to the saturation of the detector

path of these two RE propionates, significant differences were observed in the TG traces during the conversion of the anhydrous propionates into oxycarbonates. A clear two-step process is seen in the case of La-propionate decomposition in N_2 atmosphere [17], while in Ar Lu-propionate appears to decompose into $Lu_2O_2CO_3$ in a single step [19]. The further decomposition of La-oxycarbonate ($La_2O_2CO_3$ according to Kaddouri and Mazzocchia [17], $La_2O(CO_3)_2$ according to Ciontea et al. [18]) into La_2O_3 was reported to proceed without intermediate, whereas the TG traces recorded on Lu-propionate samples systematically exhibit a constant mass plateau at temperatures intermediate between the formation of $Lu_2O_2CO_3$ and its decomposition into Lu_2O_3 [19]. This plateau approximately corresponds to an overall $Lu_2O_{2.5}(CO_3)_{0.5}$ stoichiometry and appears akin to the last intermediate decomposition stage reported by Sakharova et al. [20] for $Lu(C_3H_5O_2){\cdot}2CO(NH_2)_2{\cdot}H_2O$.

The present study was undertaken to check if the thermal behaviour of Lu-propionate is a specific case or typical for heavy RE propionates. The thermal decomposition studies were performed under Ar, and the results can also be used in view of understanding the process of buffer layer manufacture in coated conductor superconducting tapes. Studies on the influence of an oxygen containing atmosphere, which are more relevant for the production of superconducting layers, will be presented elsewere.

Experimental

$Ho(CH_3COO)_3{\cdot}xH_2O$, $Er(CH_3COO)_3{\cdot}4H_2O$, $Tm(CH_3COO)_3{\cdot}xH_2O$ and $Yb(CH_3COO)_3{\cdot}xH_2O$ all from Alfa Aesar (99.9% purity (metal basis)) were dissolved in propionic acid (Alfa Aesar, 99%). After slow evaporation at room temperature without stirring, powders were obtained and used without further treatment for characterisation and for the thermal decomposition studies.

The thermogravimetry (TG) and differential thermal analysis (DTA) measurements were carried out up to 1,400 °C in a model STA 449C from Netzsch (simultaneous TG/DTA device) at a heating rate of 5 K min^{-1} in a dynamic atmosphere consisting of argon at normal pressure. The gas flow was fixed at 40 mL min^{-1}. The crucibles (6 mm diameter and 3 mm depth) were made of alumina. Buoyancy corrections were performed using data recorded on empty crucibles. The sample mass was of 11.5 ± 0.2 mg for all measurements. The powder was not

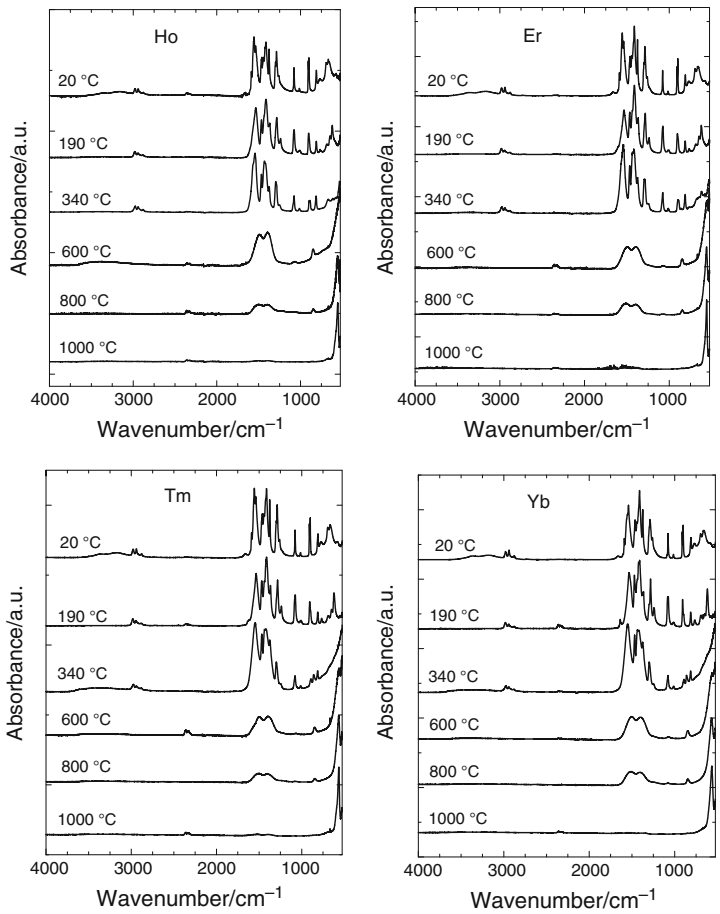

Fig. 2 FTIR spectra of the starting $Ln(C_2H_5CO_2)_3{\cdot}H_2O$ powders (20 °C) and of samples heated at 5 K min^{-1} in the DTA/TG device up to the indicated temperature and fast cooled to room temperature

compacted. α-Al_2O_3 powder (48 mg) was used as reference.

Fourier transform infra-red (FTIR) spectra of gas species evolved during decomposition were obtained with a Bruker Tensor 27 spectrometer coupled to the exhaust line of the TG/DTA device by a transfer line heated to 200 °C. The FTIR spectra were also recorded on samples heated in the TG/DTA at a rate of 5 K min^{-1} and air quenched by opening the machine (up to 700 °C) or cooled at a rate of 50 K min^{-1} (from above 700 °C) to examine the evolution of the decomposition products. The X-ray diffraction (XRD) patterns were collected on the same samples in a STOE diffractometer using Cu $K\alpha$ radiation.

Results and discussion

The XRD patterns of the powder samples after drying at room temperature are shown in Fig. 1. They are similar to the diffraction pattern of $Lu(C_2H_5CO_2)_3{\cdot}H_2O$ [19] as well as to that published by Nadzharyan et al. [21] for $Y(C_2H_5CO_2)_3{\cdot}H_2O$. Furthermore, the FTIR spectra (Fig. 2) contain the same features as those of $Lu(C_2H_5CO_2)_3{\cdot}H_2O$ [19]. As will be shown in the following, the end decomposition products are Ho_2O_3, Er_2O_3, Tm_2O_3 and Yb_2O_3, and the total relative weight losses are in very good agreement with the losses expected for the conversion of respective $Ln(C_2H_5CO_2)_3{\cdot}H_2O$ to Ln_2O_3. For each compound, measurements were replicated under the same experimental conditions on five powder samples with similar starting masses. The deviation in relative weight loss does not exceed $\pm 0.4\%$ and the temperatures, at which the different decomposition steps take place, are reproducible within 3 °C.

The TG traces recorded on the four compounds are plotted in Fig. 3 up to 1,200 °C along with the respective DTG and DTA traces. The decomposition process is characterized by three weight loss steps. The weight loss occurring between 300 and 450 °C actually covers two partially overlapping decomposition stages as will be shown in the following. The first and second weight loss steps are accompanied by sharp endothermic peaks, whereas the remaining of the decomposition process is characterized by a broad endothermic feature extending over a temperature interval extending over more than 500 °C (from about 400 °C to 1,000–1,100 °C).

The first weight loss takes place between 60 and 120 °C for all compounds. It amounts to between 4.3 ± 0.2 and

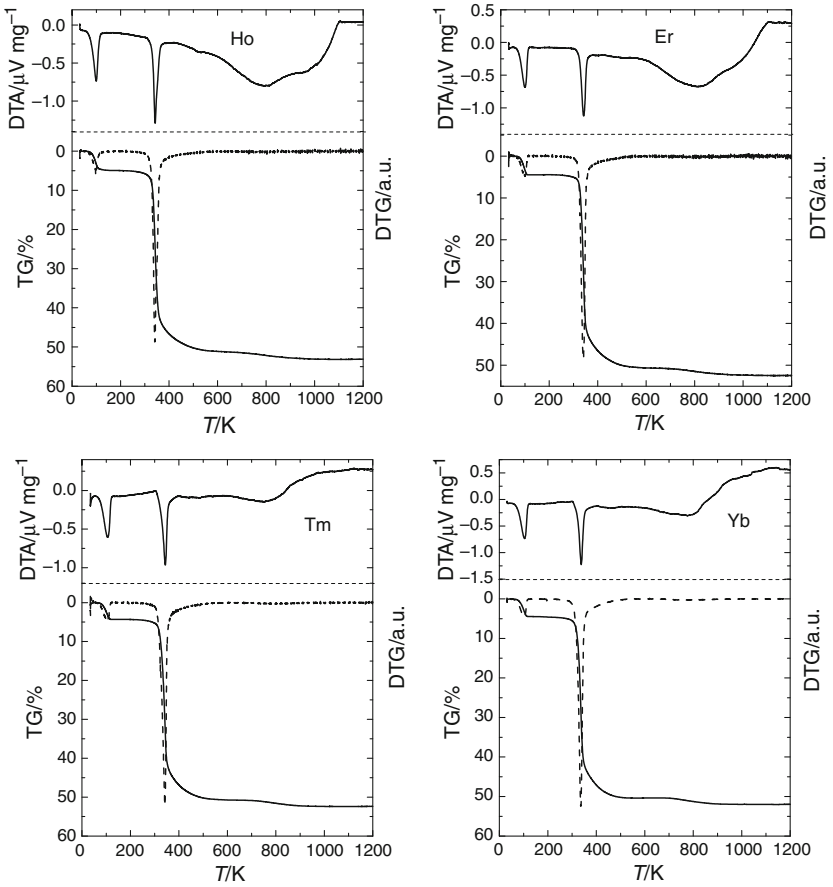

Fig. 3 TG, DTG and DTA traces recorded on $Ln(C_2H_5CO_2)_3{\cdot}H_2O$ powder samples at a heating rate of 5 K min^{-1} in flowing argon

Table 1 Experimental (exp.) and theoretical (calc.) weight losses for the four compounds under investigation

Decomposition stage	Ho-propionate		Er-propionate		Tm-propionate		Yb-propionate	
	Exp. (%)	Calc. (%)	Exp. (%)	Calc. (%)	Exp. (%)	Calc. (%)	Exp. (%)	Calc. (%)
$Ln(C_2H_5CO_2)_3{\cdot}H_2O \rightarrow Ln(C_2H_5CO_2)_3 + H_2O\uparrow$	4.9	4.5	4.5	4.5	4.3	4.4	4.5	4.4
$2Ln(C_2H_5CO_2)_3 \rightarrow Ln_2O_2CO_3 + 2CO_2\uparrow + 3C_5H_{10}O\uparrow$	47.1[a]	47.5	46.9[a]	47.3	46.6[a]	47.1	46.5[a]	46.6
$Ln_2O_2CO_3 \rightarrow (1-x)Ln_2O_2CO_3 + xLn_2O_3 + xCO_2\uparrow$	–	–	50.7	–	50.7	–	50.4	–
$(1-x)Ln_2O_2CO_3 + xLn_2O_3 \rightarrow Ln_2O_3 + (1-x)CO_2\uparrow$	53.1	53.0	52.5	52.7	52.4	52.5	52.0	52.0

The theoretical weight losses have been determined assuming $Ln(C_2H_5CO_2)_3{\cdot}H_2O$ starting stoichiometries (Ln = Ho, Er, Tm or Yb respectively)

[a] Experimental values at 400 °C

4.9 ± 0.2% of the starting sample mass depending on the lanthanide and thus corresponds well to the loss expected for a single water molecule per formula unit as evidenced in Table 1. Several FTIR spectra recorded in situ on the evolving gases during decomposition of $Ho(C_2H_5CO_2)_3{\cdot}H_2O$ are plotted in Fig. 4 and are representative for the other compounds, which all give rise to similar results. The first weight loss step is accompanied by the release of H_2O, supporting the conclusions drawn on the basis of the TG curves. In addition, the FTIR spectra recorded on powder samples quenched at 190 °C differ from those of the staring materials essentially by the disappearance of the broad absorption bands around wave numbers 3,250 and 700 cm^{-1}, which are due to H_2O (Fig. 2). On the other hand, the XRD patterns of the quenched products (Fig. 1) reveal a crystalline character with clear differences in comparison with that of the starting materials.

During the study of $Lu(C_2H_5CO_2)_3{\cdot}H_2O$ thermal decomposition [19], the main weight loss, occurring as in the present compounds between 300 and 450 °C, was found to result from two decomposition reactions: decomposition from $Lu(C_2H_5CO_2)_3$ to $Lu_2O_2CO_3$ and

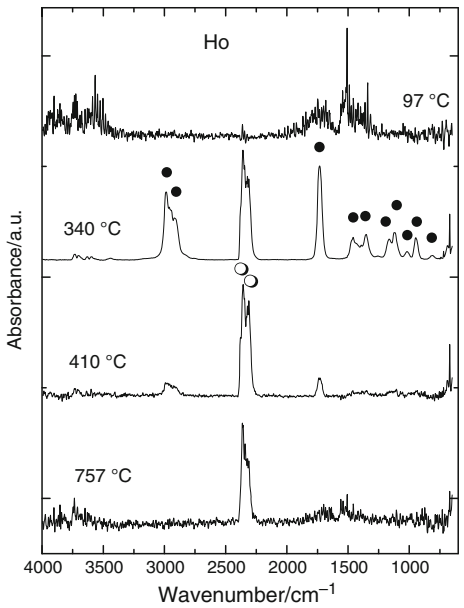

Fig. 4 FTIR spectra of the gas phase evolved from the $Ho(C_2H_5CO_2)_3{\cdot}H_2O$ sample at different temperatures during decomposition. *Open circles* CO_2, *filled circles* $C_2H_5COC_2H_5$

further decomposition of this oxycarbonate to a metastable intermediate with overall composition equivalent to $Lu_2O_{2.5}(CO_3)_{0.5}$. An approximate temperature boundary between these two events was determined at 395 °C from an inflexion in the DTG trace. In the case of $Ln(C_2H_5CO_2)_3{\cdot}H_2O$ (Ln = Ho, Er, Tm and Yb), the DTG traces do not exhibit such a feature. However, an inspection of the FTIR spectra recorded on powder samples quenched from temperatures between 320 and 400 °C (Fig. 5) reveals that the respective oxycarbonates have been formed at approximately 400 °C. Specific features of propionates like for example the CH_2 deformation band of the $–CH_2–CO–O$ group at 1,280 cm^{-1} and the CO_3^- skeletal vibration at 900 cm^{-1} progressively disappear up to 400 °C, leaving a spectrum identical with that of $Lu_2O_2CO_3{\cdot}6H_2O$ except for the absence of H_2O signature [22]. The relative weight losses at this temperature (400 °C) are in good agreement with the expected values for an oxycarbonate intermediate product (Table 1). As shown in Fig. 4 for the case of $Ho(C_2H_5CO_2)_3{\cdot}H_2O$, the gas evolved during this first part of the decomposition step consists of 3-pentanone and CO_2 (340 °C in Fig. 4). The same gas species were

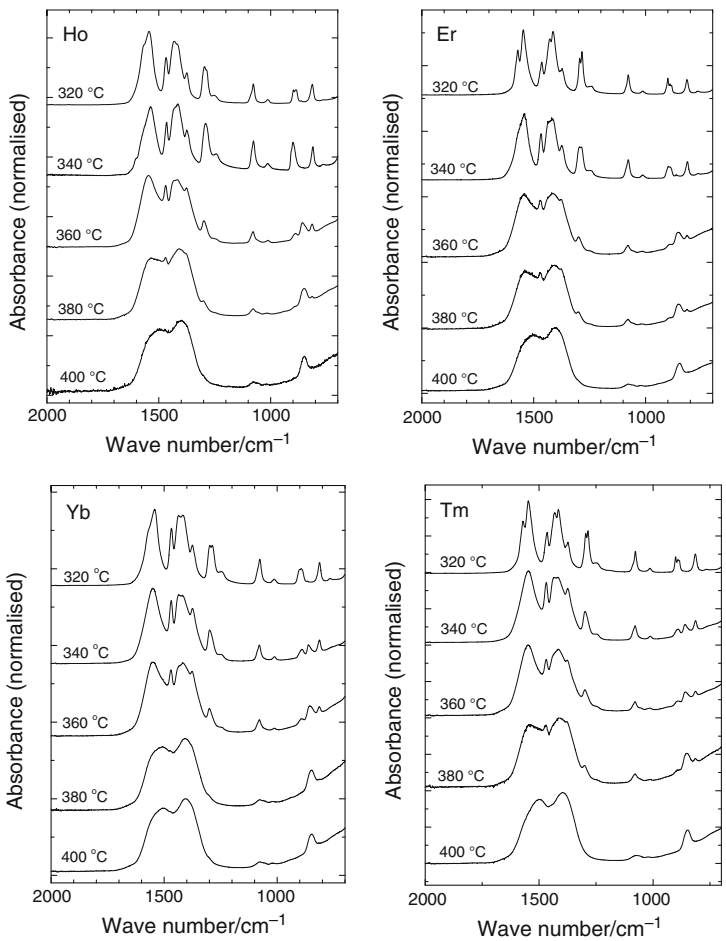

Fig. 5 FTIR spectra of solid decomposition products of $Ln(C_2H_5CO_2)_3{\cdot}H_2O$ powders heated at 5 K min^{-1} in the DTA/TG device up to the indicated temperature and air quenched to room temperature

found to be formed at this stage during the thermal decomposition of the Er-, Tm- and Yb-propionates. As shown in the XRD patterns of the quenched specimens, the samples tend to become amorphous during this process (Fig. 1).

The formation of Ho-, Er-, Tm and Yb-oxycarbonates at an intermediate stage has been observed during the thermal decomposition of several compounds including acetates [23–26], oxalates [23, 27, 28], formates [29] and malonates [30]. The formation of the oxycarbonate compounds thus appears as a frequent feature in the thermal decomposition path of metallo-organic compounds based on these heavy RE elements.

It obviously appears that the anhydrous propionates of Ho, Er, Tm and Yb undergo a thermal decomposition process similar to that of Lu [19]. This process, based on the free radical mechanism proposed by Hites and Biemann [31], involves the release of CO_2, as well as C_2H_5CO and C_2H_5 radicals that combine to form 3-pentanone ($C_2H_5COC_2H_5$) resulting in an overall reaction of the following type:

$$2Ln(C_2H_5CO_2)_3 \rightarrow 3C_2H_5COC_2H_5 + Ln_2O_2CO_3 + 2CO_2$$

This model thus accounts for the observed gas species evolving from the samples during this decomposition stage and the formation of the $Ln_2O_2CO_3$ oxycarbonate evidenced in the FTIR spectra of the decomposition product.

During studies on the thermal decomposition behaviour of Zn- and Ca-propionates, it was also observed that the dehydrated propionates release 3-pentanone upon decomposition to ZnO and $CaCO_3$[32, 33]. Although this does not appear to be a general rule since La-, Ni- and Co-propionates were reported to release mostly CO_2, CO or H_2O along with traces of CH_3CH_2COOH, CH_3CH_2OH or $CH_3CH_2CO_2$ [17, 34], it is worth noting that the recent study on La-propionate thermal decomposition published by Ciontea et al. [18] also provides evidence for the formation of 3-pentanone.

The remaining part of the second weight loss step and the third step are both accompanied by the release of CO_2 (410 and 757 °C in Fig. 4). As shown in Table 1, the total weight loss after the completion of the decomposition process fits rather well to the values theoretically expected for the full conversion of the studied $Ln(C_2H_5CO_2)_3{\cdot}H_2O$ compounds to their respective sesquioxides. The final formation of the Ln_2O_3 compounds is confirmed by XRD patterns of samples heated up to temperatures in excess of 700 °C (800 and 1,000 °C in Fig. 1). This is further supported by the FTIR spectra that present absorption bands at 555, 559, 565 and 567 cm^{-1} for the Ho, Er, Tm and Yb-based samples, respectively, in good correspondence with the values reported by McDevitt and Baun [35].

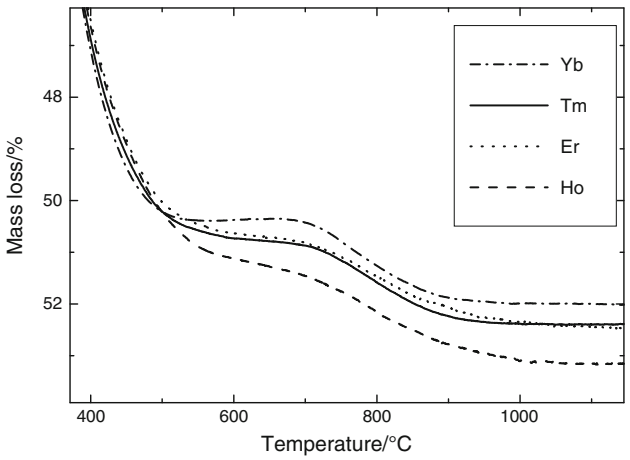

Fig. 6 Detail of the TG traces recorded on $Ln(C_2H_5CO_2)_3{\cdot}H_2O$, Ln = Ho, Er, Tm and Yb

Between the oxycarbonate and the sesquioxide stages, a nearly constant mass plateau corresponding to a 50.4–50.7% total relative weight loss extends from about 500–700 °C in the case of the Er-, Tm- and Yb-based samples, whereas a gentle weight loss slope is observed for the Ho-based sample in the same temperature interval (Fig. 6). A similar feature was observed during the thermal decomposition of Lu-propionate [19]. Although the decomposition of the Ho-, Er-, Tm- and Yb-oxycarbonates formed as intermediate products during the thermal decomposition of metallorganic compounds to oxides is often reported to take place in a single step [26–30], in many instances for both light and heavy REs, an additional intermediate stage has been reported and assigned to the formation of $Ln_2O_2(CO_3)_x{\cdot}C$ [36], $Ln_2O_3{\cdot}yCO_2$ [37], $Ln_2O_{0.6}(CO_3)_{2.4}$ [38] or $Ln_2O_{2+x}(CO_3)_{1-x}$ [39]. In particular, $Ln_2O_3{\cdot}xCO_2$ intermediates were observed during the thermal decomposition of mixed carbamide–propionate salts of Ho, Er, Tm and Yb, which have the peculiarity of proceeding via the formation of a mixture of $Ln(C_3H_5O_2)_{2.8}$ and $LnOC_3H_5O_2$ that is in turn converted into $Ln_2O_2CO_3$ [20, 40]. The lack of crystallinity of the decomposition product in the relevant temperature interval makes it difficult to identify the actual compound that forms in our samples. Taking into consideration that CO_2 evolves between the formation of the oxycarbonates and the beginning of the plateau, as well as the overall weight loss, an intermediate $Ln_2O_{2.5}(CO_3)_{0.5}$ formulation may be hypothetised. However, very broad diffraction lines corresponding to Ln_2O_3 appear in the XRD patterns already in samples quenched from 600 °C (Fig. 1) and faint absorption bands characteristic for Ln_2O_3 appear in the FTIR

spectra recorded on samples heated to temperatures between 500 and 700 °C at 5 K min^{-1} and quenched (600 °C in Fig. 2). This suggests a coexistence of $Ln_2O_2CO_3$ and Ln_2O_3 as previously suggested by Turcotte et al. [41] during a study of the thermal decomposition of RE dioxymonocarbonates.

Conclusions

Upon heating in flowing argon, $Ln(C_2H_5CO_2)_3{\cdot}H_2O$ (Ln = Ho, Er, Tm and Yb) decomposes in four stages. Around 90 °C, dehydration takes place in a single step. Decomposition of the anhydrous propionates to $Ln_2O_2CO_3$ occurs between 300 and 400 °C and is characterized by the release of CO_2 and 3-pentanone ($C_2H_5COC_2H_5$). The decomposition of $Ln_2O_2CO_3$ to Ln_2O_3 proceeds in two steps characterized by an intermediate nearly constant mass plateau corresponding to a $Ln_2O_{2.5}(CO_3)_{0.5}$ overall composition, which extends from 500 to 700 °C. The intermediate product, which stability appears to decrease with the atomic number of the RE, is probably a mixture of $Ln_2O_2CO_3$ and Ln_2O_3. The conversion of $Ln(C_2H_5CO_2)_3{\cdot}H_2O$ to Ln_2O_3 is complete at 1,100 °C. The thermal decomposition behaviour of $Ln(C_2H_5CO_2)_3{\cdot}H_2O$ (Ln = Ho, Er, Tm and Yb) is similar to that previously reported for lutetium(III) propionate hydrate and to some extent (formation of an oxycarbonate) to that of lanthanum(III) propionate.

Acknowledgements This study was supported by the Danish Agency for Science, Technology and Innovation under contract number 09-062997.

References

1. Izumi T, Shiohara Y. R&D of coated conductors for applications in Japan. Physica C. 2010;470:967–70.
2. Bhuiyan MS, Paranthaman M, Sathyamurthy S. Chemical solution-based epitaxial oxide films on biaxially textured Ni–W substrates with improved out-of-plane texture for YBCO-coated conductors. J Electron Mater. 2007;36:1270–4.
3. Lee SG, Han TS. High-T_c $YBa_2Cu_3O_{7-\delta}$ thin films fabricated from a stable acetate solution precursor. J Korean Phys Soc. 1997;31:406–9.
4. Matsubara I, Paranthaman M, Chirayil TG, Sun EY, Martin PM, Kroeger DM, Verebelyi DT, Christen DK. Preparation of epitaxial $YbBa_2Cu_3O_{7-\delta}$ on $SrTiO_3$ single crystal substrates using a solution process. Jpn J Appl Phys. 1999;38:L727–30.
5. Lee HY, Kim SI, Lee YC, Hong YP, Park YH, Ko KH. New chemical route for YBCO thin films. IEEE Trans Appl Supercond. 2003;13:2743–66.
6. Angrisani Armenio A, Augieri A, Ciontea L, Contini G, Davoli I, Galluzzi V, Mancini A, Rufoloni A, Petrisor T, Vannozzi A, Celentano G. Characterization of epitaxial $YBa_2Cu_3O_{7-\delta}$ films deposited by metal propionate precursor solution. Supercond Sci Technol. 2008;21:125015 (7 pp).
7. Ciontea L, Angrisani A, Celentano G, Petrisor T Jr, Rufoloni A, Vannozzi A, Augieri A, Galuzzi V, Mancini A, Petrisor T. Metal propionate synthesis of epitaxial $YBa_2Cu_3O_{7-x}$ films. J Phys Conf Ser. 2008;97:012302 (6 pp).
8. Angrisani Armenio A, Celentano G, Rufoloni A, Vannozzi A, Augieri A, Galluzzi V, Mancini A, Ciontea L, Petrisor T, Contini G, Davoli I. Deposition and characterisation of metal propionate derived epitaxial $YBa_2Cu_3O_{7-x}$ films for coated conductor fabrication. IEEE Trans Appl Supercond. 2009;19:3204–7.
9. Knoth K, Schlobach B, Hühne R, Schultz L, Holzapfel B. $La_2Zr_2O_7$ and Ce–Gd–O buffer layers for YBCO coated conductors using chemical solution deposition. Physica C. 2005; 426–431:979–84.
10. Hassini A, Pomar A, Ruyter A, Roma N, Puig T, Obradors X. Conducting $La_{0.7}Sr_{0.3}MnO_3$-superconducting $YBaCu_3O_7$ epitaxial bilayers grown by chemical solution deposition. Physica C. 2007;460–462:1357–8.
11. Chen HS, Kumar RV, Glowacki BA. Study on chemical-solution-deposited lanthanum zirconium oxide film based on the Taguchi method. J Sol–Gel Sci Technol. 2009;51:102–11.
12. Zhao Y, Suo HL, Grivel JC, Ye S, Liu M, Zhou ML. Study on $Ce_xLa_{1-x}O_2$ buffer layer used in coated conductors by chemical solution method. J Inorg Mater. 2009;24:1201–4.
13. Larbalestier D, Gurevich A, Feldmann DM, Polyanskii A. High-T_c superconducting materials for electric power applications. Nature. 2001;414:368–77.
14. Coll M, Pomar A, Puig T, Obradors X. Atomically flat surface: the key issue for solution-derived epitaxial multilayers. Appl Phys Exp 2008;1:121701 (3 pp).
15. Kaddouri A, Mazzocchia C, Tempesti E, Nomen R, Sempere J. Sol-gel processing of copper-chromium catalysts for ester hydrogenation. J Therm Anal. 1009;53:533–45.
16. Gobert-Ranchoux E, Charbonnier F. Comportement thermique des propionates hydrates de calcium, strontium et barium. J Therm Anal. 1977;12:33–42.
17. Kaddouri A, Mazzocchia CJ. Thermoanalytic study of some metal propionates synthesised by sol-gel route: a kinetic and thermodynamic study. J Anal Appl Pyrolysis. 2002;65:253–67.
18. Ciontea L, Nasui M, Petrisor T Jr, Mos RB, Gabor MS, Varga RA, Petrisor T. Synthesis, crystal structure and thermal decomposition of $[La_2(CH_3CH_2COO)_6{\cdot}(H_2O)_3]{\cdot}3.5H_2O$ precursor for high-*k* La_2O_3 thin films deposition. Mater Res Bull. 2010;45: 1203–8.
19. Grivel JC. Thermal decomposition of lutetium propionate. J Anal Appl Pyrolysis. 2010;89:250–4.
20. Sakharova YG, Bogodukhova TI, Evtushenko IY, Loginov VI. Thermal decomposition of carbamide compounds of thulium, ytterbium and lutetium propionates. Z Neorg Khim. 1979;24: 323–30.
21. Nadzharyan K, Mlynskaya V, Magunov R. LiC_2H_5COO–$Y(C_2H_5COO)_3$–H_2O system at 25 °C. Russ J Inorg Chem (Engl Transl). 1984;29:1797–9.
22. Liu S, Ma RJ. Synthesis of hydrated lutetium carbonate. Acta Chem Scand. 1997;51:893–5.
23. Hussein GAM, Balboul BAA. Ytterbium oxide from different precursors: formation and characterization. Thermoanalytical studies. Powder Technol. 1999;103:156–64.
24. Hussein GAM, Mekhemer GAH, Balboul BAA. Formation and surface characterization of thulium oxide catalysts. Phys Chem Chem Phys. 2000;2:2033–8.
25. Hussein GAM, Balboul BAA, Mekhemer GAH. Holmium oxide from holmium acetate, formation and characterization: thermoanalytical studies. J Anal Appl Pyrolysis. 2000;56:263–72.
26. Mahfouz RM, Al-Shehri SM, Monshi MAS, Alhaizan AI, Abd El-Salam NM. Isothermal decomposition of γ-irradiated erbium acetate. Radiat Eff Defects Solids. 2007;162:95–100.

27. Balboul BAA. Thermal decomposition study of erbium oxalate hexahydrate. Thermochim Acta. 2000;351:55–60.
28. Glasner A, Levy E, Steinberg M. Thermal decomposition of ytterbium oxalate. J Inorg Nucl Chem. 1964;26:1143–9.
29. Masuda Y. Thermal decomposition of formates. Part IX. Thermal decomposition of rare earth formate anhydrides. Thermochim Acta. 1983;67:271–85.
30. Muraishi K, Yokobayashi H, Nagase K. Systematics on the thermal reactions of lanthanide malonates $Ln_2(C_3H_2O_4)_3{\cdot}nH_2O$ in the solid state. Thermochim Acta. 1991;182:209–17.
31. Hites A, Biemann K. On the mechanism of ketonic decarboxylation. Pyrolysis of calcium decanoate. J Am Chem Soc. 1972;94: 5772–7.
32. Barnes PA, Stephenson G, Warrington SB. The use of TA–GLC–MS as a quantitative specific EGA technique for the investigation of complex thermal decomposition reactions: the thermal decomposition of calcium propanoate. J Therm Anal. 1982;25: 299–311.
33. Skoršepa J, Godočíkova E, Černák J. Comparison on thermal decomposition of propionate, benzoate and their chloroderivative salts of Zn(II). J Therm Anal Calorim. 2004;75:773–80.
34. El Baydi M, Poillerat G, Rehspringer JL, Gautier JL, Koenig JF, Charlier P. A sol-gel route for the preparation of Co_3O_4 catalyst for oxygen electrocatalysis in alkaline medium. J Solid State Chem. 1994;109:281–8.
35. McDevitt NT, Baun WL. Infrared absorption study of metal oxides in the low frequency region (700–240 cm^{-1}). Spectrochim Acta. 1964;20:799–808.
36. Dododzhanov MA, Komarov VP, Shaplygin IS. Thermal decomposition of dysprosium, holmium, erbium and ytterbium abietates. Zh Neorg Khim. 1986;31:640–2.
37. Nagashima K, Wakita H, Mochizuki A. The synthesis of crystalline rare earth carbonates. Bull Chem Soc Jpn. 1973;46:152–6.
38. Glasner A, Steinberg M. Thermal decomposition of the light rare earth oxalates. J Inorg Nucl Chem. 1961;22:39–48.
39. Moscardini D'Assunção L, Giolito I, Ionashiro M. Thermal decomposition of the hydrated basic carbonates of lanthanides and yttrium. Thermochim Acta. 1989;137:319–30.
40. Sakharova YG, Bogodukhova TI, Loginov VI, Evtushenko IY. Thermal decomposition of carbamide compounds of terbium, dysprosium, holmium, erbium and yttrium propionates. Z Neorg Khim. 1978;23:2953–8.
41. Turcotte RP, Sawyer JO, Eyring L. On the rare earth dioxymonocarbonates and their decomposition. Inorg Chem. 1969; 8:238–46.